Fetal Diagnosis and Therapy

Original Paper

Fetal Diagn Ther 2020;47:665–674
DOI: 10.1159/000507619

Received: August 5, 2019
Accepted: March 25, 2020
Published online: June 25, 2020

MicroRNA-148b-3p and MicroRNA-25-3p Are Overexpressed in Fetuses with Late-Onset Fetal Growth Restriction

José Morales-Roselló[a, b] José Luis García-Giménez[c, d]
Llucia Martinez Priego[e] Daymé González-Rodríguez[c] Salvador Mena-Mollá[c, d]
Angel Maquieira Catalá[f] Gabriela Loscalzo[a] Silvia Buongiorno[a]
Vaidile Jakaite[a] Antonio José Cañada Martínez[g] Alfredo Perales Marín[a, b]

[a]Servicio de Obstetricia, Hospital Universitario y Politécnico La Fe, Valencia, Spain; [b]Departamento de Pediatría, Obstetricia y Ginecología, Universidad de Valencia, Valencia, Spain; [c]EpiDisease SL, and Consortium Center for Biomedical Network Research on Rare Diseases (CIBERER), Institute of Health Carlos III, Valencia, Spain; [d]Departamento de Fisiología, Universidad de Valencia, Valencia, Spain; [e]Servicio de Secuenciación, Fundación para el Fomento de la Investigación Sanitaria y Biomédica de la Comunidad valenciana (FISABIO), Valencia, Spain; [f]Departamento de Química, Universidad Politécnica de Valencia, Valencia, Spain; [g]Unidad de Bioestadística, Instituto de Investigación Sanitaria La Fe, Valencia, Spain

Keywords
Doppler ultrasound · Late-onset fetal growth restriction · MicroRNA · miR-148b-3p · miR-25-3p · Schwann cells

Abstract
Objective: It was the aim of this study to describe a microRNA (miRNA) profile characteristic of late-onset fetal growth restriction (FGR) and to investigate the pathways involved in their biochemical action. ***Methods:*** In this prospective study, 25 fetuses (16 normal and 9 with FGR [estimated fetal weight <10th centile plus cerebroplacental ratio <0.6765 multiples of the median]) were evaluated with Doppler ultrasound after 36 weeks. Afterwards, for every fetus, plasma from umbilical vein blood was collected at birth, miRNA was extracted, and full miRNA sequencing was performed. Subsequently, comparisons were done in order to obtain those miRNAs that were differentially expressed. ***Results:*** The FGR fetuses expressed upregulation of two miRNAs: miR-25-3p and, especially, miR-148b-3p, a miRNA directly involved in Schwann cell migration, neuronal plasticity, and energy metabolism ($p = 0.0072$, $p = 0.0013$). ***Conclusions:*** FGR fetuses express a different miRNA profile, which includes overexpression of miR-25-3p and miR-148b-3p. This information might improve our understanding of the pathophysiological processes involved in late-onset FGR. Future validation and feasibility studies will be required to propose miRNAs as a valid tool in the diagnosis and management of FGR.

Introduction

Fetal growth restriction (FGR) occurs when a fetus fails to reach its growth potential [1]. Its importance lies in its association with a higher probability of perinatal morbidity and mortality and the subsequent long-term neurologic and cardiovascular consequences in adult life [2, 3]. FGR comprises two varieties: early-onset FGR (<34 weeks) is less frequent and is characterized by the existence of placental disease, deceleration of fetal growth, and progressive hemodynamic dysfunction, typically af-

karger@karger.com
www.karger.com/fdt

José Morales-Roselló
Servicio de Obstetricia, Hospital Universitario y Politécnico La Fe
Avenida Fernando Abril Martorell 106
ES–46026 Valencia (Spain)
jose.morales@uv.es

fecting in its onset the uterine and umbilical Doppler examination, while late-onset FGR (>34 weeks) is more frequent and is defined by the unbalance between fetal demands and placental supply, resulting in the detection of a characteristic low cerebroplacental ratio (CPR) regardless of the estimated fetal weight (EFW) [4]. Late-onset FGR tends to be subtle. However, despite what might be thought, it is especially harmful, as it leads to frequently undiagnosed suboptimal arborization and brain underdevelopment [5, 6].

Unfortunately, an adverse perinatal outcome (APO) in fetuses with late-onset FGR is difficult to predict. Clinical protocols may use the CPR or a combination of the CPR and EFW for its identification. However, this methodology has a poor accuracy and cannot be applied clinically yet [7–10]. Hopefully, this prediction could be theoretically improved using diverse biochemical markers, a search that has become of crucial importance.

MicroRNAs (miRNAs) are small RNA sequences, on average 22 nucleotides in length [11], with the ability to regulate gene expression in different organisms. Their action is mediated through the inhibition of translation or the promotion of mRNA degradation [12]. Their genes are encoded within the genome, suggesting that their transcription might be coordinated with the transcription of other genes. In summary, generation of the mature miRNA molecule involves the processing of a primary miRNA transcript in the nucleus to obtain the final product in the cell cytosol, a small single RNA strand which participates in a variety of cellular processes (development, proliferation, function, and differentiation) and in the pathogenesis of many human diseases [13]. miRNAs can target genes with relative specificity. To date, about 2,500 miRNA sequences are known in humans (miRBase v21) [14], and it was predicted that 30–80% of the human genes may be influenced by at least one miRNA [15, 16]. Interestingly, recent studies have shown that miRNAs are also expressed in the placenta, suggesting a potential regulatory role in its development [17]. In addition, some miRNAs have been described to be hypoxia-regulated and associated with FGR [18].

The purpose of the current study was to define a miRNA profile characteristic of late-onset FGR, investigating the pathways involved in their biochemical action.

Subjects and Methods

Patient Recruitment and Doppler Examination

This was a prospective study of 25 fetuses at the tertiary public maternity La Fe Hospital. These fetuses underwent an ultrasound examination between 36 and 40 weeks that included biometry and EFW calculation plus a Doppler evaluation of the umbilical artery (UA) and middle cerebral artery (MCA) pulsatility indices (PIs). The UA and MCA were examined using color and pulsed Doppler ultrasound according to earlier descriptions [19, 20], and the CPR was calculated as the simple ratio between the MCA PI and the UA PI [21].

All babies were delivered within 15 days or less after the scan, and only the last examination per fetus was included in the analysis. In order to adjust for the effect of gestational age (GA), EFW, and birth weight (BW), the values were converted into local reference centiles [22] adjusted only for fetal gender. Also, CPR values were converted into multiples of the median (MoM), dividing each value by the 50th centile at each GA as previously described [19]. CPR medians (50th centile) were represented by the equation

$$\text{CPR 50th centile} = -3.814786276 + 0.36363249 \times GA - 0.005646672 \times GA^2,$$

where "GA" was the GA in weeks with decimals.

All Doppler examinations were performed by the first author (J.M.-R.), a teaching expert in obstetric ultrasound certified by the Spanish Society of Obstetrics and Gynecology, using General Electric Voluson® (E8/E6/730) ultrasound machines (General Electric Healthcare, Spain) with 2- to 8-MHz convex probes during fetal quiescence, in the absence of fetal tachycardia, and keeping the insonation angle relative to the examined vessels as small as possible and always below 30°.

GA was determined according to the crown-rump length in the 1st trimester. Multiple pregnancies and those complicated by congenital fetal abnormalities or aneuploidies were excluded. Gestational characteristics including parity, number of gestations, and maternal ethnicity, age, weight and height were collected at examination, together with the indicated ultrasound parameters. Labor outcome data including BW, BW centile, mode of delivery, 5-min Apgar score, cord arterial pH, and date of admission to the neonatal care unit were also collected at birth.

Ponderal and Hemodynamic Characteristics of the Groups Studied

For the purpose of comparison, the study included two different types of fetus: late-onset FGR fetuses, with an abnormal EFW (<10th centile) and an abnormal CPR (<0.6765 MoM), and normal fetuses, with a normal EFW (>10th centile) and a normal CPR (>0.6765 MoM) [19]. Fetuses with intermediate features (abnormal CPR with normal EFW or normal CPR with abnormal EFW) were not considered.

Sample Collection and Small RNA Extraction and Quantification

After birth, plasma samples from the fetal umbilical vein and maternal peripheral blood were collected in EDTA tubes and centrifuged at 3,500 rpm for 10–15 min. Once plasma had been obtained, each sample was stored at –80 °C until small RNA extraction. While maternal plasma was stored for future research, 500 µL of fetal blood plasma were used to isolate cell-free total RNA (including miRNAs) using the miRNeasy Serum/Plasma kit (Qiagen, Valencia, CA, USA) following the manufacturer's protocol. The RNA was eluted with 25 µL of RNase-free water. The concentration of cell-free total RNA (including miRNAs) was quantified us-

ing NanoDrop ND 2000 UV spectrophotometer (Thermo Fisher Scientific, Wilmington, DE, USA).

Library Preparation and Next-Generation Sequencing

Small RNA libraries were generated and indexed using a modified Illumina TruSeq small RNA protocol. In this modified protocol, the libraries were size selected (range 90–170 bp) using a Blue Pippin instrument (Sage Science, Beverly, MA, USA). A positive RNA control was included (Thermo Fisher Scientific Human Brain Total RNA catalog #AM7962). Single-end sequencing was performed on an Illumina NextSeq platform on High-Output 1 × 50 bp Run (NextSeq 500/550 High-Output v2 75 cycles kit, FC-404-2005).

Differential Expression Analysis

The first step was to assess the quality of the Illumina raw sequences with the FastQC software (https://www.bioinformatics.babraham.ac.uk/projects/fastqc/). Based on the results obtained, the sequence reads were trimmed to remove sequencing adapters and low-quality bases using the software Cutadapt (http://cutadapt.readthedocs.org/en/stable/). Once the data were deemed of sufficient quality, they were mapped against the human GRCh38 build reference sequence, taken from Ensembl. After that, an intersection between the aligned position of reads and the miRNA coordinates taken from miRBase v21 was performed. The alignment and quantification steps were performed using the Subread and Rsubread packages [23, 24].

A multidimensional scaling plot was used to get a closer look at how samples were distributed according to the miRNA expression values. miRNAs with very low counts across all libraries provide little evidence for differential expression. We filtered out these miRNAs prior to further analysis. Subsequently, the trimmed mean of M-values normalization method (TMM normalization) [25] was performed to eliminate composition biases between libraries. We also estimated the specific dispersions per gene with a negative binomial distribution [26, 27].

Group Comparisons

After miRNA had been extracted and sequencing performed, comparisons were done between the group of late-onset FGR fetuses and the group of normal fetuses (control group). As previously indicated, late-onset FGR was considered when abnormal values of CPR [19, 28] plus abnormal values of BW [22] were present. Conversely, normality was considered if both parameters were within normal range. As per the local protocol, all fetuses were subsequently managed according to their progression in labor, including intrapartum fetal heart rate assessment, which was interpreted according to the FIGO guidelines [29]. All study comparisons were performed using the Mann-Whitney test for continuous data and Fisher's exact test for categorical data. Significance was considered with $p < 0.05$.

Prediction of miRNA Targets and Overrepresentation Analysis

We first used DIANA-microT-CDS, accessed from the DIANA web server [30]. This tool showed whether the target was also predicted by miRanda or TargetScan or was experimentally validated in TarBase v7.0. We used the DIANA-miRPath v3.0 functional analysis online suite to identify miRNAs controlling significant molecular pathways annotated on the Kyoto Encyclopedia of Genes and Genomes (KEGG), using the following default parameters: experimentally supported interactions from DIANA TarBase v.7.0; a p value threshold of 0.001; and a microT threshold of 0.8. To reduce the number of false-positive miRNA targets, we applied a false discovery rate (FDR) correction to selected KEGG pathways. The algorithm used in this analysis was a one-tailed Fisher exact test [31].

Results

Descriptive Statistics of the Study Population

The study included 25 fetuses, of whom 14 (56%) were male and 11 (44%) were female, all of them being of Spanish Caucasian origin. Online supplementary Figure 1 (see www.karger.com/doi/10.1159/000507619 for all online suppl. material) shows the distribution of measurements according to the CPR MoM and BW centile [8, 19, 28]. Nine fetuses had late-onset FGR (abnormal CPR plus abnormal BW values), while 16 were fetuses with normal hemodynamic and ponderal features (normal CPR plus normal BW).

In Table 1 we compare the normal with the FGR pregnancies. In summary, the mothers in the FGR group were thinner than those in the normal group, and the fetuses had a lower CPR MoM, EFW, EFW centile, BW, and BW centile ($p < 0.001$). In addition, when compared with the fetuses with a normal outcome, the FGR fetuses were delivered earlier ($p = 0.04$).

Identification of Differentially Expressed miRNAs by Small RNA-Seq

Table 2 shows the initial comparison between normal and FGR fetuses regarding the differential expression analysis of upregulated and downregulated miRNAs. For accuracy and selection purposes, only miRNAs with the criterion of FDR <0.05 were included. In comparison with the normal fetuses, the FGR fetuses showed a total of four initially differentially expressed miRNAs: miR-148b-3p, miR-25-3p and miR-16-5p, which were upregulated, as well as miR-1910-5p, which was downregulated. miR-148b-3p had by far the highest significance. As a matter of caution, we discarded miR-16-5p due to its relation to hemolysis, which might always be present in blood samples to some degree [32, 33]. Figure 1 shows the heat map of the miRNA expression profile with the miRNAs selected in Table 2. The cluster was done on the basis of $\log_2$ (expression level in treatment/expression level in control). Yellow denotes downregulation of miRNAs and red denotes upregulation of miRNAs in blood samples from the neonatal cord.

Fetal Diagn Ther 2020;47:665–674
DOI: 10.1159/000507619

Table 1. Descriptive statistics of the two groups studied: normal and FGR fetuses

	Normal fetuses (n = 16)		FGR fetuses (n = 9)		p value
	mean (SD)	median (1st, 3rd Q), range	mean (SD)	median (1st, 3rd Q), range	
Maternal age, years	33.4 (4.6)	33.5 (29.25, 36), 27–41	34.2 (5.04)	34 (29.5, 38.5), 27–42	0.73
Gestations, n	1.87 (1.1)	2 (1, 2), 1–5	1.89 (1.36)	1 (1, 2.5), 1–5	0.78
Parity	0.62 (0.72)	0.5 (0, 1), 0–2	0.67 (0.87)	0 (0, 1.5), 0–2	0.98
Maternal weight, kg[a]	65.56 (11.35)	67 (53.5, 73), 52–86	51.7 (8.2)	51 (48, 55), 40–67	0.01
Maternal height, cm[b]	163.8 (10.5)	168 (156, 171), 144–176	161.7 (2.5)	162 (160, 164), 158–165	0.38
GA at examination, weeks	39.4 (1)	39.6 (38.7, 40.2), 36.7–40.4	38.3 (1.4)	38.1 (37.0, 39.4), 36.7–40.7	0.08
EFW Hadlock-4, g	3,547 (441.5)	3,505 (3,161, 4,013), 2,830–4,246	2,491 (456)	2,500 (2,134, 2,763), 1,810–3,373	<0.001
EFW Local Pop. Ref. centiles	70.44 (27.2)	78 (47.25, 95.25), 21–99	7.2 (10.3)	4 (0.5, 11), 0–32	<0.001
CPR, MoM	1.56 (0.28)	1.49 (1.42, 1.73), 1.01–2.1	0.48 (0.11)	0.51 (0.37, 0.58), 0.31–0.59	<0.001
GA at labor, weeks	40.14 (1.08)	40.6 (39.3, 41), 37.9–41.4	38.75 (1.5)	38.86 (37.4, 40.1), 36.9–41	0.04
Interval examination-labor, days	5.44 (3.6)	4.5 (3, 8), 1–15	3 (2.34)	2 (1, 5), 0–7	0.87
BW, g	3,610 (467.9)	3,500 (3,320, 3,823), 3,000–4,700	2,381 (324.7)	2,350 (2,118, 2,665), 1,845–2,800	<0.001
BW Local Pop. Ref. centiles	62.25 (26.3)	61 (37.7, 91.7), 29–100	1.78 (1.39)	2 (0.5, 3), 0–4	<0.001
	n (%)		n (%)		p value
Gender					0.22
Male	7 (43.7%)		7 (77.8%)		
Female	9 (56.3%)		2 (22.2%)		
BW <10th Local Pop. Ref. centiles	0 (0%)		9 (100%)		–
5-min Apgar score <7	0 (0%)		0 (0%)		–
Arterial cord pH <7.20[c]	3 (18.7%)		2 (22.2%)		0.78
Ethnicity					–
Caucasian	16 (100%)		9 (100%)		
Non-Caucasian	0 (0%)		0 (0%)		
Smokers[d]	0 (0%)		1 (11.1%)		–
Onset of labor					0.93
Induction of labor	6 (37.5%)		8 (88.9%)		
Spontaneous onset of labor	6 (37.5%)		0 (0%)		
Cesarean section (abnormal CTG)	0 (0%)		0 (0%)		
Cesarean section (elective)	4 (25%)		1 (11.1%)		
Mode of delivery					0.95
Spontaneous vaginal delivery	9 (56.3%)		4 (44.4%)		
Assisted vaginal delivery	1 (6.25%)		1 (11.1%)		
Cesarean section (abnormal CTG)	1 (6.25%)		3 (33.3%)		
Cesarean section (dystocia)	5 (31.2%)		1 (11.1%)		
Admission to neonatal unit					0.054
No	16 (100%)		7 (77.8%)		
Yes	0 (0%)		2 (22.2%)		

FGR, fetal growth restriction; SD, standard deviation; Q, quartiles; GA, gestational age; EFW, estimated fetal weight; CPR, cerebroplacental ratio; MoM, multiples of the median; BW, birth weight; Local Pop. Ref. centiles, centiles according to local population references (Hospital Clinic de Barcelona, Spain population references); CTG, cardiotocography. [a] Data were missing on 7 and 2 patients, respectively. [b] Data were missing on 6 and 2 patients, respectively. [c] Data were missing on 1 patient in each group. [d] Data were missing on 7 patients and 1 patient, respectively.

Table 2. Differential miRNA expression between FGR and normal fetuses

miRNA	logFC	logCPM	*F*	*p* value	FDR
hsa-miR-148b-3p	2.913109	6.392020	23.88636	7.813586e–06	0.003484859
hsa-miR-16-5p	1.639640	12.972890	18.11788	7.311848e–05	0.016305421
hsa-miR-1910-5p	–4.069241	0.916709	15.22769	2.465907e–04	0.036659814
hsa-miR-25-3p	1.339374	11.323960	14.20868	3.726486e–04	0.041550317

FGR, fetal growth restriction; logFC, logarithm with the base of 2 of the fold change – a negative logFC value corresponds to a downregulated miRNA and a positive logFC value means that the miRNA is upregulated relative to the reference condition; logCPM, logarithm with the base of 2 of the counts per million reads obtained by the miRNA; *F*, the value of the statistic test; FDR, *p* corrected value with false discovery rate.

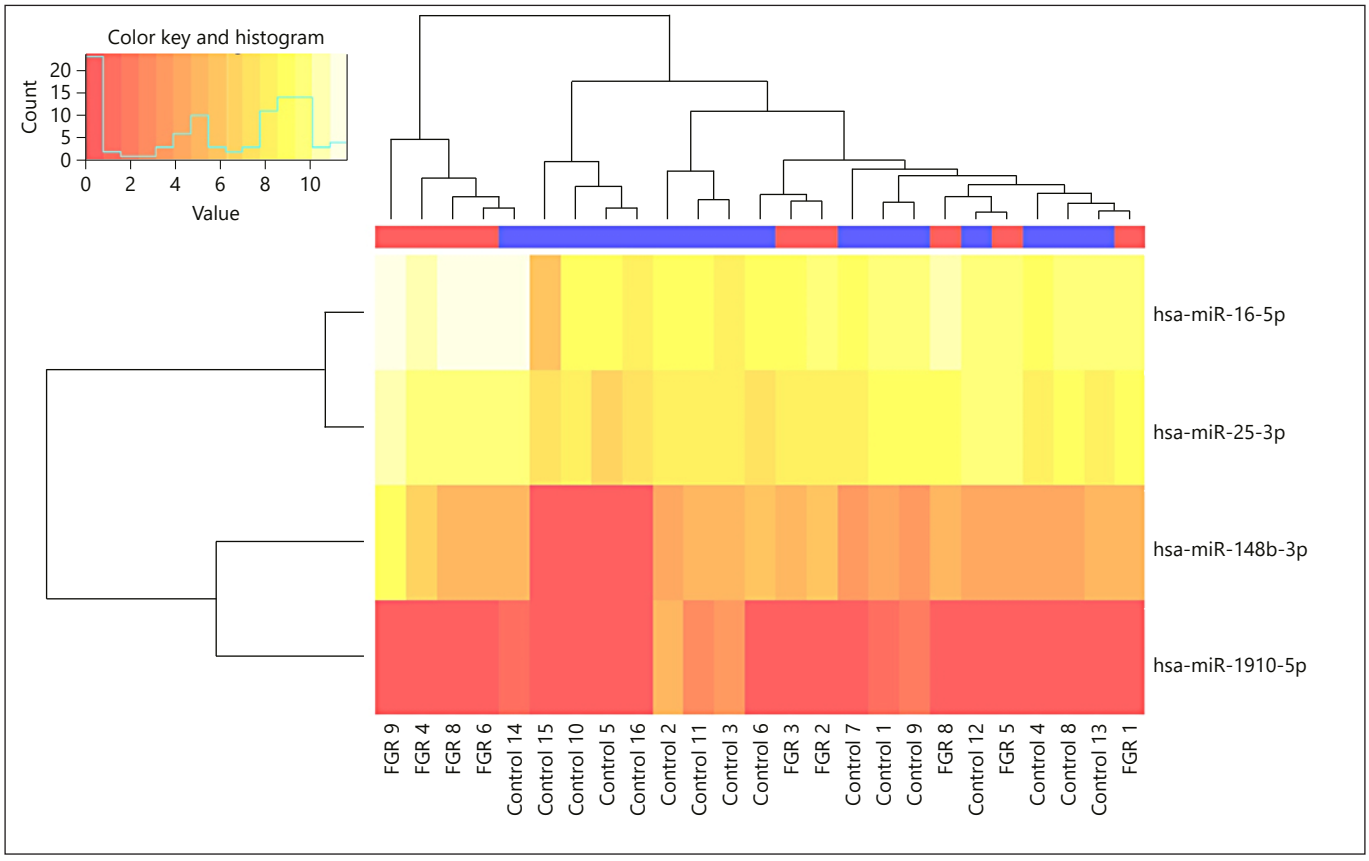

Fig. 1. Heat map with the hierarchical clustering of differentially expressed miRNAs in fetuses with late-onset fetal growth restriction (FGR) (red) versus normal fetuses (blue) according the expression levels of the miRNAs miR-1910-5p, miR-148b-3p, miR-16-5p, and miR-25-3p.

Comparison of the Logarithm of Counts per Million Reads

Figure 2 shows box-and-whisker plots representing the logarithm of counts per million reads (logCPM) of those miRNAs that presented significant differences: miR-148b-3p and miR-25-3p (Mann-Whitney $p < 0.05$). It is noteworthy to underline that a difference existed between the differential expression analysis of upregulated and downregulated miRNAs and the individual statistical analysis performed between normal and FGR fetuses concerning the logCPM. When the analysis of differential expression was done, four miRNAs were significant with

Table 3. Selected KEGG pathways regulated by the differentially expressed miRNAs miR-25-3p and miR-148b-3p in FGR vs. normal fetuses

KEGG pathway	*p* value	Genes	miRNAs
Prion diseases	7.31985499212e–15	5	miR-148b-3p and miR-25-3p
Fatty acid biosynthesis	3.52242071263e–13	2	miR-148b-3p
Oocyte meiosis	1.27759516409e–05	31	miR-148b-3p and miR-25-3p
Cell cycle	1.7071934491e–05	42	miR-148b-3p and miR-25-3p
Viral carcinogenesis	1.7071934491e–05	45	miR-148b-3p and miR-25-3p
Lysine degradation	3.01715187799e–05	14	miR-148b-3p and miR-25-3p
Estrogen signaling pathway	0.00028055720575	26	miR-148b-3p and miR-25-3p
p53 signaling pathway	0.000316939071553	24	miR-148b-3p and miR-25-3p
FoxO signaling pathway	0.000929050869461	37	miR-148b-3p and miR-25-3p
Protein processing in endoplasmic reticulum	0.000929050869461	42	miR-148b-3p and miR-25-3p
Adherens junction	0.00183745694845	19	miR-148b-3p and miR-25-3p
Long-term depression	0.00183745694845	15	miR-148b-3p and miR-25-3p
Proteoglycans in cancer	0.0019678042498	42	miR-148b-3p and miR-25-3p
Steroid biosynthesis	0.00292457111324	4	miR-148b-3p
Hippo signaling pathway	0.00292457111324	34	miR-148b-3p and miR-25-3p
Valine, leucine, and isoleucine biosynthesis	0.00360593689391	2	miR-25-3p
Hepatitis B	0.00373563003963	35	miR-148b-3p and miR-25-3p
Progesterone-mediated oocyte maturation	0.00574829839216	26	miR-148b-3p and miR-25-3p
cGMP-PKG signaling pathway	0.00675142184669	40	miR-148b-3p and miR-25-3p
Prostate cancer	0.0079060270266	25	miR-148b-3p and miR-25-3p
Endometrial cancer	0.0100040376492	15	miR-148b-3p and miR-25-3p
Non-small cell lung cancer	0.0100700510791	15	miR-148b-3p and miR-25-3p
Chronic myeloid leukemia	0.0129054369882	21	miR-148b-3p and miR-25-3p
Sphingolipid signaling pathway	0.0131352576976	27	miR-148b-3p and miR-25-3p
Colorectal cancer	0.015375047919	16	miR-148b-3p and miR-25-3p
Glioma	0.015375047919	17	miR-148b-3p and miR-25-3p
Sulfur metabolism	0.0155260139399	2	miR-148b-3p
Thyroid cancer	0.0263000781158	9	miR-148b-3p and miR-25-3p
RNA degradation	0.0440095764865	21	miR-148b-3p and miR-25-3p

Pathways obtained by miRPath v3.0 were ordered according to *p* value. Genes: number of genes from that pathway regulated by some of significant differentially expressed miRNAs in FGR vs. normal fetuses. miRNAs: number of differentially expressed miRNAs in FGR vs. normal fetuses implied in that pathway [30]. FGR, fetal growth restriction.

an FDR <0.05 (Table 2). However, when the logCPM comparison was performed in an independent way and without considering the expression of all those miRNAs that contributed to the differential expression analysis, only miR-148b-3p and miR-25-3p turned out to be finally statistically significant (Fig. 2). Therefore, only these were finally selected to explore relevant pathways related to FGR.

Analysis of miRNA Targets and Biochemistry Pathways in the Context of FGR

All miRNAs had a large number of potential target sites, so we explored those of relevance to FGR. Interestingly and in agreement with Figure 2, miR-1910-5p did not release any pathway. Therefore, miR-16-5p and miR-1910-5p where finally removed from the analysis. In order to clarify the role of the remaining miRNAs miR-148b-3p and miR-25-3p in FGR, we analyzed the biochemical networks in which they participate. We carried out a DIANA-miRPath v3.0 analysis and KEGG pathway analysis to look for any significantly enriched pathway. A total of 29 pathways with an FDR <0.05 were retrieved (Table 3). Some of them are related to lipid metabolism, such as biosynthesis of fatty acids [31] and sphingolipids [34], crucial for neuronal tissue development, while others are related to protein processing in the endoplasmic reticulum [35] or to protein metabolism, such as biosynthesis of branched-chain amino acids valine, leucine, and isoleucine [36].

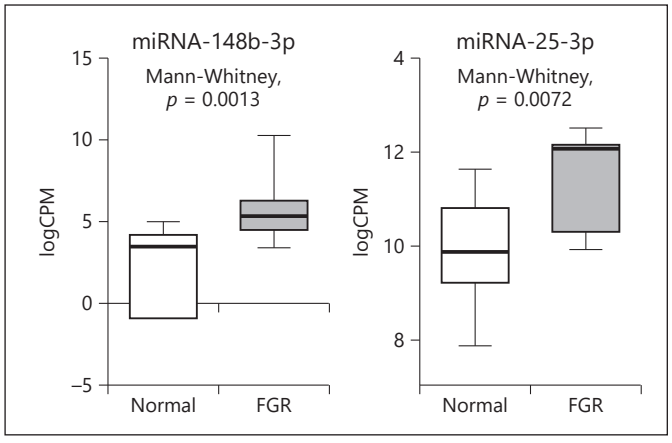

Fig. 2. Box plots representing the logarithm of counts per million reads (logCPM) of the circulating miRNAs miR-148b-3p and miR-25-3p in late-onset fetal growth restriction (FGR) fetuses compared to normal fetuses. Whiskers represent the 10th and 90th centiles.

Discussion

Principal Findings

Analyzing circulating miRNAs from neonatal cord blood and using next-generation sequencing we found that miR-148b-3p and miR-25-3p were upregulated in late-onset FGR fetuses. This different miRNA profile is a novel finding that might improve our understanding of late-onset growth compromise.

Research Implications

CPR MoM has emerged as the best marker of APO at the end of pregnancy [37–40]; however, its accuracy as a single parameter or in association with EFW centile and other clinical parameters is not good enough to obtain clinically reliable results [8]. As a consequence, new biochemical markers are being investigated in order to obtain accurate predictions of APO and neurocognitive dysfunction.

In recent years, the focus has shifted to miRNAs. These molecules behave like fine tuners in the regulation of gene expression and are crucial for many biological processes [41]. A large number of the more than 1,000 miRNAs discovered in humans are related to pregnancy and are produced by the placenta and the uterus in normal and pathological conditions. They exert their action locally in a paracrine fashion, or distally released as exosomes in maternal blood, regulating fetal and maternal homeostasis [41]. Moreover, several studies have shown that altered expression of the miRNome in maternal circulation or in placental tissue may reflect gestational disorders such as preeclampsia, spontaneous abortion, preterm birth, low BW, or macrosomia [42].

Role in Neuronal Plasticity

miR-148b seems to have special relevance in diverse molecular mechanisms related to neuronal hypoxia, neurogenesis, and neuronal metabolism and development. Particularly, miR-148b-3p upregulation promoted Schwann cell (SC) migration, whereas silencing of miR-148b-3p inhibited SC migration in vitro [43]. The molecular background of miR-148b-3p is in fact very interesting. It belongs to the miR-148/152 family [44], which includes miR-148a, miR-148b, and miR-152 and is considered a placenta-associated miRNA, which means it is expressed ubiquitously [43], not only in the placenta but also in other tissues. However, as indicated, the most interesting issue concerning its role in fetal medicine is its ability to promote the growth of SCs, responsible for myelin formation. miR-148-3p plays a role in the regeneration of peripheral nerves by regulating SC migration via targeting cullin-associated NEDD8-dissociated protein 1 (Cand1). Overexpression of miR-148-3p enhanced the migratory ability of SCs, while inhibition attenuated SC migration in vitro [43]. These effects occur in unison with other miRNAs such as miR-132, miR-210, miRNA sc-3, miR-221, and miR-222, which also increase the migratory ability of SCs, and miRNA sc-8, miR-9, miR-98, miR-1, and miR-182, which diminish this ability [45].

A parallel may therefore be drawn between peripheral nerve repair and axonal development (arborization) in the central nervous system. A good example of this is miR-132, which apart from promoting peripheral nerve repair mediated by SCs, as indicated, has been found to protect the central nervous system: miR-132 controls dendritic plasticity [46] and is required for normal dendrite maturation in newborn neurons [47]. Therefore, miR-132 functions as a key activity-dependent regulator of cognition, whose expression must be maintained within a limited range to ensure normal learning and memory formation [48]. In fact, miR-132 has been considered as a master regulator of neuronal health [49], and its supplementation is being evaluated for the treatment of diseases such as tau-associated neurodegenerative disorders [50]. Therefore, in an analogous way, miR-148b-3p might also play a role in the protection of the central nervous system. In theory, as brain tissue depends on myelination, miR-148b-3p might contribute to the protection of brain tissue under different circumstances, such as in chronic hypoxia [51].

Role in Energy Production

The possible role of miR-148b-3p in the protection of SCs might have a relationship to a number of biochemical functions. Regarding carbohydrates, miR-148b inhibits hypoxia-induced elevation of lactate production and hypoxia-induced increase in glucose consumption, thereby reducing cellular growth [52]. Regarding amino acids and proteins, miR-148b-3p and miR-25-3p behave as key regulators of biosynthesis of valine, leucine, and isoleucine and also regulate protein processing at the endoplasmic reticulum, both pathways of special relevance to fetal growth during the last trimester of pregnancy [35, 36] and during periods of nutritional deprivation [53]. Finally, regarding fatty acid metabolism, both miR-25-3p and miR-148b-3p control biosynthesis of fatty acids and sphingolipids [31, 34, 54], essential molecules for stem cell differentiation morphogenesis and embryo development [54] that are also related to preeclampsia and FGR [55, 56].

Clinical Implications

A practical result of the differential expression of miR-25-3p and miR-148b-3p in fetal blood would be the possibility to detect them also in maternal blood in order to develop clinical diagnostic tests. Hypoxia-related miRNAs produced in the placenta have been detected in maternal blood [57]. In this regard, if miRNAs are able to cross the placental barrier and circulate between the mother and the fetus [39], miR-148b-3p and miR-25-3p might also be detected in maternal serum and become markers of APO in an isolated or combined way, consequently improving the accuracy of late-onset FGR diagnosis.

Strengths and Limitations

The strengths of this study are, first, its novelty, as we have been the first investigators to perform full sequencing of all miRNAs in fetal blood, and, second, the finding of a miRNA profile directly related to neuronal development. Some shortcomings, however, might be the absence of validation in a different population, the paucity of follow-up data, and the absence of data related to neurocognitive evolution in childhood.

Conclusions

FGR fetuses express a different miRNA profile, which includes overexpression of miR-25-3p and, especially, miR-148b-3p, miRNAs related to cellular metabolism and neuronal plasticity. Future work is needed to assess the levels of miR-148b-3p and miR-25-3p in maternal serum in order to evaluate if they could improve the understanding and management of late-onset FGR, helping in the prediction of neurocognitive disability.

Acknowledgements

We thank the midwifes and the personnel of the maternity operating rooms for their contribution during the collection of blood samples.

Statement of Ethics

The research complies with the guidelines for human studies and was conducted ethically in accordance with the World Medical Association Declaration of Helsinki. Institutional review board permission was obtained for this work (Ref. No. 2016/053). All patients gave written informed consent to participate in the study.

Conflict of Interest Statement

J.L. García-Giménez and S. Mena-Mollá own stocks in EpiDisease SL, an epigenetics company focused on the development of epigenetic biomarkers. The other authors report no conflicts of interest.

Funding Sources

Funds were obtained from several sources: (1) the iPlacenta project, European Union's Horizon 2020 Research and Innovation Programme, Marie Skłodowska-Curie grant agreement No. 765274; (2) VLC-Biomed Grant, Universidad de Valencia and Universidad Politécnica de Valencia; (3) Clinical Study Protocol X213220 Xoma, Hospital Universitario y Politécnico La Fe; and (4) Charity Run "9 km 9 meses," Instituto de Investigación Sanitaria La Fe and Ayuntamiento de Torrente, Valencia, Spain.

Author Contributions

J. Morales-Roselló designed the study, performed the ultrasound examinations, and wrote the manuscript. J.L. García-Giménez, L. Martinez Priego, D. González-Rodríguez, S. Mena-Mollá, and A. Maquieira Catalá made the genetic analysis, supervised the final manuscript, and suggested valuable inputs to the text. G. Loscalzo, S. Buongiorno, and V. Jakaite performed the data search and made notable contributions to the final text. A.J. Cañada Martínez performed part of the statistical analysis. A. Perales Marín supervised the manuscript and suggested valuable inputs to the text.

References

1 American College of Obstetricians and Gynecologists. ACOG Practice bulletin No. 134: fetal growth restriction. Obstet Gynecol. 2013 May;121(5):1122–33.
2 Lees C, Marlow N, Arabin B, Bilardo CM, Brezinka C, Derks JB, et al.; TRUFFLE Group. Perinatal morbidity and mortality in early-onset fetal growth restriction: cohort outcomes of the trial of randomized umbilical and fetal flow in Europe (TRUFFLE). Ultrasound Obstet Gynecol. 2013 Oct;42(4):400–8.
3 Yzydorczyk C, Armengaud JB, Peyter AC, Chehade H, Cachat F, Juvet C, et al. Endothelial dysfunction in individuals born after fetal growth restriction: cardiovascular and renal consequences and preventive approaches. J Dev Orig Health Dis. 2017 Aug;8(4):448–64.
4 Figueras F, Gratacós E. Update on the diagnosis and classification of fetal growth restriction and proposal of a stage-based management protocol. Fetal Diagn Ther. 2014;36(2):86–98.
5 Miller SL, Huppi PS, Mallard C. The consequences of fetal growth restriction on brain structure and neurodevelopmental outcome. J Physiol. 2016 Feb;594(4):807–23.
6 Quezada S, Castillo-Melendez M, Walker DW, Tolcos M. Development of the cerebral cortex and the effect of the intrauterine environment. J Physiol. 2018 Dec;596(23):5665–74.
7 Triunfo S, Crispi F, Gratacos E, Figueras F. Prediction of delivery of small-for-gestational-age neonates and adverse perinatal outcomes by fetoplacental Doppler at 37 weeks' gestation. Ultrasound Obstet Gynecol. 2017;49(3):364–71.
8 Morales-Roselló J, Khalil A, Fornés-Ferrer V, Perales-Marín A. Accuracy of the fetal cerebroplacental ratio for the detection of intrapartum compromise in nonsmall fetuses. J Matern Fetal Neonatal Med. 2019 Sep;32(17):2842–52.
9 Bligh LN, Alsolai AA, Greer RM, Kumar S. Cerebroplacental ratio thresholds measured within 2 weeks before birth and risk of Cesarean section for intrapartum fetal compromise and adverse neonatal outcome. Ultrasound Obstet Gynecol. 2018 Sep;52(3):340–6.
10 Bligh LN, Alsolai AA, Greer RM, Kumar S. Prelabor screening for intrapartum fetal compromise in low-risk pregnancies at term: cerebroplacental ratio and placental growth factor. Ultrasound Obstet Gynecol. 2018 Dec;52(6):750–6.
11 Carthew RW, Sontheimer EJ. Origins and mechanisms of miRNAs and siRNAs. Cell. 2009 Feb;136(4):642–55.
12 Bartel DP. MicroRNAs: target recognition and regulatory functions. Cell. 2009 Jan;136(2):215–33.
13 Ichihara A, Jinnin M, Yamane K, Fujisawa A, Sakai K, Masuguchi S, et al. MicroRNA-mediated keratinocyte hyperproliferation in psoriasis vulgaris. Br J Dermatol. 2011 Nov;165(5):1003–10.
14 Vlachos IS, Paraskevopoulou MD, Karagkouni D, Georgakilas G, Vergoulis T, Kanellos I, et al. DIANA-TarBase v7.0: indexing more than half a million experimentally supported miRNA:mRNA interactions. Nucleic Acids Res. 2015 Jan;43(Database issue):D153–9.
15 Lewis BP, Burge CB, Bartel DP. Conserved seed pairing, often flanked by adenosines, indicates that thousands of human genes are microRNA targets. Cell. 2005 Jan;120(1):15–20.
16 Friedman RC, Farh KK, Burge CB, Bartel DP. Most mammalian mRNAs are conserved targets of microRNAs. Genome Res. 2009 Jan;19(1):92–105.
17 Hayder H, O'Brien J, Nadeem U, Peng C. MicroRNAs: crucial regulators of placental development. Reproduction. 2018 Jun;155(6):R259–71.
18 Mouillet JF, Chu T, Hubel CA, Nelson DM, Parks WT, Sadovsky Y. The levels of hypoxia-regulated microRNAs in plasma of pregnant women with fetal growth restriction. Placenta. 2010 Sep;31(9):781–4.
19 Morales-Roselló J, Khalil A, Morlando M, Hervás-Marín D, Perales-Marín A. Doppler reference values of the fetal vertebral and middle cerebral arteries, at 19–41 weeks gestation. J Matern Fetal Neonatal Med. 2015 Feb;28(3):338–43.
20 Acharya G, Wilsgaard T, Berntsen GK, Maltau JM, Kiserud T. Reference ranges for serial measurements of umbilical artery Doppler indices in the second half of pregnancy. Am J Obstet Gynecol. 2005 Mar;192(3):937–44.
21 Baschat AA, Gembruch U. The cerebroplacental Doppler ratio revisited. Ultrasound Obstet Gynecol. 2003 Feb;21(2):124–7.
22 Figueras F, Meler E, Iraola A, Eixarch E, Coll O, Figueras J, et al. Customized birthweight standards for a Spanish population. Eur J Obstet Gynecol Reprod Biol. 2008 Jan;136(1):20–4.
23 Liao Y, Smyth GK, Shi W. The Subread aligner: fast, accurate and scalable read mapping by seed-and-vote. Nucleic Acids Res. 2013 May;41(10):e108.
24 Liao Y, Smyth GK, Shi W. featureCounts: an efficient general purpose program for assigning sequence reads to genomic features. Bioinformatics. 2014 Apr;30(7):923–30.
25 Robinson MD, Oshlack A. A scaling normalization method for differential expression analysis of RNA-seq data. Genome Biol. 2010;11(3):R25.
26 Robinson MD, Smyth GK. Small-sample estimation of negative binomial dispersion, with applications to SAGE data. Biostatistics. 2008 Apr;9(2):321–32.
27 Robinson MD, Smyth GK. Moderated statistical tests for assessing differences in tag abundance. Bioinformatics. 2007 Nov;23(21):2881–7.
28 Morales-Roselló J, Khalil A, Morlando M, Papageorghiou A, Bhide A, Thilaganathan B. Changes in fetal Doppler indices as a marker of failure to reach growth potential at term. Ultrasound Obstet Gynecol. 2014 Mar;43(3):303–10.
29 Ayres-de-Campos D, Spong CY, Chandraharan E; FIGO Intrapartum Fetal Monitoring Expert Consensus Panel. FIGO consensus guidelines on intrapartum fetal monitoring: cardiotocography. Int J Gynaecol Obstet. 2015 Oct;131(1):13–24.
30 Vlachos IS, Zagganas K, Paraskevopoulou MD, Georgakilas G, Karagkouni D, Vergoulis T, et al. DIANA-miRPath v3.0: deciphering microRNA function with experimental support. Nucleic Acids Res. 2015 Jul;43 W1:W460–6.
31 Crawford MA. The role of essential fatty acids in neural development: implications for perinatal nutrition. Am J Clin Nutr. 1993 May;57(5 Suppl):703S–9S.
32 Shah JS, Soon PS, Marsh DJ. Comparison of methodologies to detect low levels of hemolysis in serum for accurate assessment of serum microRNAs. PLoS One. 2016 Apr;11(4):e0153200.
33 Kirschner MB, Edelman JJ, Kao SC, Vallely MP, van Zandwijk N, Reid G. The impact of hemolysis on cell-free microRNA biomarkers. Front Genet. 2013 May;4:94.
34 Olsen AS, Færgeman NJ. Sphingolipids: membrane microdomains in brain development, function and neurological diseases. Open Biol. 2017 May;7(5):170069.
35 Metcoff J, Wikman-Coffelt J, Yoshida T, Bernal A, Rosado A, Yoshida P, et al. Energy metabolism and protein synthesis in human leukocytes during pregnancy and in placenta related to fetal growth. Pediatrics. 1973 May;51(5):866–77.
36 Mogami H, Yura S, Itoh H, Kawamura M, Fujii T, Suzuki A, et al. Isocaloric high-protein diet as well as branched-chain amino acids supplemented diet partially alleviates adverse consequences of maternal undernutrition on fetal growth. Growth Horm IGF Res. 2009 Dec;19(6):478–85.
37 Morales-Roselló J, Khalil A. Fetal cerebral redistribution: a marker of compromise regardless of fetal size. Ultrasound Obstet Gynecol. 2015 Oct;46(4):385–8.
38 Morales-Roselló J, Khalil A, Morlando M, Bhide A, Papageorghiou A, Thilaganathan B. Poor neonatal acid-base status in term fetuses with low cerebroplacental ratio. Ultrasound Obstet Gynecol. 2015 Feb;45(2):156–61.

39 Khalil AA, Morales-Roselló J, Elsaddig M, Khan N, Papageorghiou A, Bhide A, et al. The association between fetal Doppler and admission to neonatal unit at term. Am J Obstet Gynecol. 2015 Jul;213(1):57.e1–7.
40 Khalil AA, Morales-Roselló J, Morlando M, Hannan H, Bhide A, Papageorghiou A, et al. Is fetal cerebroplacental ratio an independent predictor of intrapartum fetal compromise and neonatal unit admission? Am J Obstet Gynecol. 2015 Jul;213(1):54.e1–10.
41 Cai M, Kolluru GK, Ahmed A. Small molecule, big prospects: microRNA in pregnancy and its complications. J Pregnancy. 2017; 2017:6972732.
42 Barchitta M, Maugeri A, Quattrocchi A, Agrifoglio O, Agodi A. The role of miRNAs as biomarkers for pregnancy outcomes: a comprehensive review. Int J Genomics. 2017; 2017:8067972.
43 Qian TM, Zhao LL, Wang J, Li P, Qin J, Liu YS, et al. miR-148b-3p promotes migration of Schwann cells by targeting cullin-associated and neddylation-dissociated 1. Neural Regen Res. 2016 Jun;11(6):1001–5.
44 Friedrich M, Pracht K, Mashreghi MF, Jäck HM, Radbruch A, Seliger B. The role of the miR-148/-152 family in physiology and disease. Eur J Immunol. 2017 Dec;47(12):2026–38.
45 Sohn EJ, Park HT. MicroRNA mediated regulation of Schwann cell migration and proliferation in peripheral nerve injury. BioMed Res Int. 2018 Apr;2018:8198365.
46 Wayman GA, Davare M, Ando H, Fortin D, Varlamova O, Cheng HY, et al. An activity-regulated microRNA controls dendritic plasticity by down-regulating p250GAP. Proc Natl Acad Sci USA. 2008 Jul;105(26):9093–8.
47 Magill ST, Cambronne XA, Luikart BW, Lioy DT, Leighton BH, Westbrook GL, et al. MicroRNA-132 regulates dendritic growth and arborization of newborn neurons in the adult hippocampus. Proc Natl Acad Sci USA. 2010 Nov;107(47):20382–7.
48 Hansen KF, Karelina K, Sakamoto K, Wayman GA, Impey S, Obrietan K. miRNA-132: a dynamic regulator of cognitive capacity. Brain Struct Funct. 2013 May;218(3):817–31.
49 Wood H. MicroRNA-132 – master regulator of neuronal health? Nat Rev Neurol. 2018 Sep; 14(9):508–9.
50 El Fatimy R, Li S, Chen Z, Mushannen T, Gongala S, Wei Z, et al. MicroRNA-132 provides neuroprotection for tauopathies via multiple signaling pathways. Acta Neuropathol. 2018 Oct;136(4):537–55.
51 Ortega SB, Kong X, Venkataraman R, Savedra AM, Kernie SG, Stowe AM, et al. Perinatal chronic hypoxia induces cortical inflammation, hypomyelination, and peripheral myelin-specific T cell autoreactivity. J Leukoc Biol. 2016 Jan;99(1):21–9.
52 Ding X, Liu J, Liu T, Ma Z, Wen D, Zhu J. miR-148b inhibits glycolysis in gastric cancer through targeting SLC2A1. Cancer Med. 2017 Jun;6(6):1301–10.
53 Liechty EA, Lemons JA. Protein metabolism in the fetal-placental unit. In: Cowett RM, editor. Principles of perinatal-neonatal metabolism. New York, USA: Springer; 1991. p. 276–90.
54 Wang G, Bieberich E. Morphogenetic sphingolipids in stem cell differentiation and embryo development. In: Pébay A, Wong RCB, editors. Lipidomics of stem cells. Stem cell biology and regenerative medicine. Springer International AG; 2017. Chapter 2.
55 Charkiewicz K, Goscik J, Blachnio-Zabielska A, Raba G, Sakowicz A, Kalinka J, et al. Sphingolipids as a new factor in the pathomechanism of preeclampsia – mass spectrometry analysis. PLoS One. 2017 May;12(5):e0177601.
56 Davison JM, Homuth V, Jeyabalan A, Conrad KP, Karumanchi SA, Quaggin S, et al. New aspects in the pathophysiology of preeclampsia. J Am Soc Nephrol. 2004 Sep;15(9):2440–8.
57 Whitehead CL, Teh WT, Walker SP, Leung C, Larmour L, Tong S. Circulating microRNAs in maternal blood as potential biomarkers for fetal hypoxia in-utero. PLoS One. 2013 Nov; 8(11):e78487.